Differential Faraday rotation and polarimetric SAR

Semyon Tsynkov[1]

[1]Department of Mathematics
North Carolina State University, Raleigh, NC

2018 AFOSR Electromagnetics Contractors Meeting
January 9–11, 2018, Arlington, VA

Collaborator and Support

- Collaborator:
  - Dr. Mikhail Gilman (Research Assistant Professor, NCSU)
- Support:
  - AFOSR Program in Electromagnetics, Dr. Arje Nachman

Motivation

- PolSAR images are obtained in four scattering channels:
  - Determined by polarization of the transmitted and scattered wave.
- PolSAR provides more information about the target.
- Transionospheric SAR is prone to distortions caused by plasma.
- Faraday rotation (FR) is a rotation of the polarization plane:
  - Due to gyrotropy of ionospheric plasma in the geomagnetic field;
  - Affects both transmitted and scattered signals as they propagate.
- If the FR angle is known, then the effect of FR on SAR is mitigated by a linear transformation applied to the four imaging channels:
  - Assuming that every part of the signal is rotated by the same angle.
- However, the FR angle is a function of the propagating frequency:
  - Different parts of the signal are rotated by different angles (twisting);
  - This effect will be called the differential Faraday rotation (dFR).

Polarimetric matched filter (PMF)

- For the variation of FR angle $\sim \pi$, the polarization information is compromised, and traditional correction becomes inadequate:
  - Image distortions due to dFR/twisting can be substantial.
- Polarimetric matched filter (PMF) addresses the twisting effect:
  - Takes into account all channels at the signal processing stage;
  - Contrary to the traditional approach that does the post-processing.
- PMF essentially eliminates image distortions due to dFR.
- Coupled processing of channels has been introduced previously [Voccola 2013], [Wright 2003], although not in the context of dFR.
- FR may have an adverse effect on single-polarization SAR as well:
  - Difficulties related to amplitude variation and poor conditioning of reconstruction.
- Quad-pol case, which is a more comprehensive imaging scenario, also allows for a more efficient solution of the dFR problem.

Faraday rotation (FR) in a homogeneous plasma

- Monochromatic linearly polarized incident EM wave with no FR (from the antenna at $\boldsymbol{x}$ to the target at $\boldsymbol{z}$):

$$\begin{pmatrix} E^{\mathsf{i}}_{\mathsf{H}} \\ E^{\mathsf{i}}_{\mathsf{V}} \end{pmatrix}(t,\boldsymbol{z}) = e^{-i\omega(t-R_z/v_{\text{ph}})} \begin{pmatrix} E^{\mathsf{i}}_{\mathsf{H}} \\ E^{\mathsf{i}}_{\mathsf{V}} \end{pmatrix}(t,\boldsymbol{x}), \quad \text{where} \quad R_z = |\boldsymbol{z}-\boldsymbol{x}|.$$

- FR is a slow rotation of the polarization plane:

$$\varphi_{\mathsf{F}} = -\frac{R_z}{2c}\frac{\omega_{\text{pe}}^2 \Omega_{\mathsf{e}} \cos\beta}{\omega^2}, \quad \text{where} \quad \omega_{\text{pe}}^2 = \frac{4\pi N_{\mathsf{e}} e^2}{m_{\mathsf{e}}}, \quad \Omega_{\mathsf{e}} = -\frac{e|\boldsymbol{H}_0|}{m_{\mathsf{e}} c},$$

and β is the angle between the propagation direction and $\boldsymbol{H}_0$.

- Propagation with FR:

$$\begin{pmatrix} E^{\mathsf{i}}_{\mathsf{H}} \\ E^{\mathsf{i}}_{\mathsf{V}} \end{pmatrix}(t,\boldsymbol{z}) = e^{-i\omega(t-R_z/v_{\text{ph}})}\mathbf{R}(\varphi_{\mathsf{F}}) \cdot \begin{pmatrix} E^{\mathsf{i}}_{\mathsf{H}} \\ E^{\mathsf{i}}_{\mathsf{V}} \end{pmatrix}(t,\boldsymbol{x}),$$

where $\mathbf{R}$ is the rotation matrix: $\mathbf{R}(\varphi_{\mathsf{F}}) = \begin{pmatrix} \cos\varphi_{\mathsf{F}} & \sin\varphi_{\mathsf{F}} \\ -\sin\varphi_{\mathsf{F}} & \cos\varphi_{\mathsf{F}} \end{pmatrix}$.

Scattering by a point target

- Point target at $\boldsymbol{z}$ with the scattering matrix $\mathbf{S}$:

$$\begin{pmatrix} E_{\mathsf{H}}^{\mathsf{s}} \\ E_{\mathsf{V}}^{\mathsf{s}} \end{pmatrix}(t,\boldsymbol{z}) = \begin{pmatrix} S_{\mathsf{HH}} & S_{\mathsf{HV}} \\ S_{\mathsf{VH}} & S_{\mathsf{VV}} \end{pmatrix} \cdot \begin{pmatrix} E_{\mathsf{H}}^{\mathsf{i}} \\ E_{\mathsf{V}}^{\mathsf{i}} \end{pmatrix}(t,\boldsymbol{z}).$$

- Propagation back to the antenna at $\boldsymbol{x}$:

$$\begin{pmatrix} E_{\mathsf{H}}^{\mathsf{s}} \\ E_{\mathsf{V}}^{\mathsf{s}} \end{pmatrix}(t,\boldsymbol{x}) = e^{-i\omega(t-2R_z/v_{\mathrm{ph}})}\mathbf{R}(\varphi_{\mathsf{F}}) \cdot \mathbf{S} \cdot \mathbf{R}(\varphi_{\mathsf{F}}) \cdot \begin{pmatrix} E_{\mathsf{H}}^{\mathsf{i}} \\ E_{\mathsf{V}}^{\mathsf{i}} \end{pmatrix}(t,\boldsymbol{x}).$$

- Data matrix $\mathbf{M}$ — response to two basic linear polarizations:

$$\mathbf{M}(t) = \begin{pmatrix} M_{\mathsf{HH}} & M_{\mathsf{HV}} \\ M_{\mathsf{VH}} & M_{\mathsf{VV}} \end{pmatrix} = e^{-i\omega(t-2R_z/v_{\mathrm{ph}})}\mathbf{R}(\varphi_{\mathsf{F}}) \cdot \mathbf{S} \cdot \mathbf{R}(\varphi_{\mathsf{F}}).$$

- As $\mathbf{R}(\varphi_1+\varphi_2) = \mathbf{R}(\varphi_1)\cdot\mathbf{R}(\varphi_2)$, we obtain the reconstruction:

$$\mathbf{S} = e^{i\omega(t-2R_z/v_{\mathrm{ph}})}\mathbf{R}(-\varphi_{\mathsf{F}}) \cdot \mathbf{M}(t) \cdot \mathbf{R}(-\varphi_{\mathsf{F}}).$$

  Valid even when incident and scattered field are ≈orthogonal.
- Idealized case: R_z, ω_{pe}, $\boldsymbol{H}_0$ need to be known.

Polarimetric imaging in 1D

- Interrogating waveforms are linear frequency modulated (LFM) pulses, i.e., chirps:

$$\begin{pmatrix} E_{\mathrm{H}}^{\mathrm{i}} \\ E_{\mathrm{V}}^{\mathrm{i}} \end{pmatrix}_{(\mathrm{H,V})} (t,x) = \boldsymbol{E}_{(\mathrm{H,V})} A(t) e^{-i\omega_0 t},$$

where the two basic polarizations, horizontal and vertical, are

$$\boldsymbol{E}_{(\mathrm{H})} = \begin{pmatrix} E_0 \\ 0 \end{pmatrix} \quad \text{and} \quad \boldsymbol{E}_{(\mathrm{V})} = \begin{pmatrix} 0 \\ E_0 \end{pmatrix},$$

and the chirp envelope is

$$A(t) = \chi_\tau(t) e^{-i\alpha t^2}, \quad \chi_\tau(t) = \begin{cases} 1, & t \in [-\tau/2, \tau/2], \\ 0, & \text{otherwise.} \end{cases}$$

- Instantaneous frequency for LFM signals:

$$\omega(t) = \omega_0 + 2\alpha t = \omega_0 + \frac{B}{\tau} t, \quad |t| \le \frac{\tau}{2},$$

where α is the chirp rate and $B = 2\alpha\tau$ is the bandwidth.

Incident field

- The signals propagate parallel to the magnetic field: $\cos\beta = \pm 1$.
- The propagation is dispersive and subject to FR:

$$\begin{pmatrix} E^{\mathrm{i}}_{\mathsf{H}} \\ E^{\mathrm{i}}_{\mathsf{V}} \end{pmatrix}_{(\mathsf{H},\mathsf{V})} (t,z) = A_\delta(t - R_z/v_{\mathrm{gr}}(\omega_0)) e^{-i\omega_0(t - R_z/v_{\mathrm{ph}}(\omega_0))} \mathbf{R}(\breve{\varphi}_{\mathsf{F}}) \cdot \boldsymbol{E}_{(\mathsf{H},\mathsf{V})},$$

where

$$A_\delta(t) = \chi_{\tau-\delta\tau}(t) e^{-i(\alpha+\delta\alpha)t^2}, \quad \delta\tau = \frac{B}{\omega_0}\frac{R_z}{c}\frac{\omega_{\mathrm{pe}}^2}{\omega_0^2}, \quad \delta\alpha = \alpha\frac{\delta\tau}{\tau},$$

and

$$v_{\mathrm{ph}} = \sqrt{\omega_{\mathrm{pe}}^2 + k^2c^2}/k, \quad v_{\mathrm{gr}} = kc^2/\sqrt{\omega_{\mathrm{pe}}^2 + k^2c^2}, \quad k = \sqrt{\omega^2 - \omega_{\mathrm{pe}}^2}/c.$$

The velocities do not depend on $\boldsymbol{H}_0$ because $|\Omega_{\mathsf{e}}| \ll \omega_{\mathrm{pe}} \ll \omega_0$.
- The FR angle for LFM signals is no longer constant — dFR:

$$\breve{\varphi}_{\mathsf{F}}(t,z) = -\frac{R_z}{2c}\frac{\omega_{\mathrm{pe}}^2 \Omega_{\mathsf{e}}}{\omega^2(t - R_z/v_{\mathrm{gr}}(\omega_0))}.$$

Single-pulse image of a point target

- The received signal:

$$\mathbf{M}(t) = e^{-i\omega_0 \mathfrak{t}_{\mathrm{ph}}(t,z)} A_{2\delta}(\mathfrak{t}_{\mathrm{gr}}(t,z))\mathbf{R}(\varphi_{\mathsf{F}}(t,z)) \cdot \mathbf{S} \cdot \mathbf{R}(\varphi_{\mathsf{F}}(t,z)),$$

  where

$$\mathfrak{t}_{\mathrm{ph,gr}}(t,z) = t - 2R_z/v_{\mathrm{ph,gr}}(\omega_0) \quad \text{and} \quad \varphi_{\mathsf{F}}(t,\boldsymbol{z}) = -\frac{R_z}{2c}\frac{\omega_{\mathrm{pe}}^2 \Omega_{\mathsf{e}}}{\omega^2(\mathfrak{t}_{\mathrm{gr}}(t,z))}.$$

- The reconstruction of the scattering matrix:

$$\mathbf{S} = e^{i\omega_0 \mathfrak{t}_{\mathrm{ph}}(t,z)} \overline{A_{2\delta}(\mathfrak{t}_{\mathrm{gr}}(t,z))}\mathbf{R}(-\varphi_{\mathsf{F}}(t,z)) \cdot \mathbf{M}(t) \cdot \mathbf{R}(-\varphi_{\mathsf{F}}(t,z)).$$

  The right-hand side does not depend on t (by substitution of $\mathbf{M}$).
- $\mathbf{S}$ can be obtained from $\mathbf{M}(t)$ $\forall t$ such that $|\mathfrak{t}_{\mathrm{gr}}(t,z)| \leqslant (\tau - 2\delta\tau)/2$.
- Using the entire interval, we obtain the image:

$$\mathbf{I} = \int e^{i\omega_0 \mathfrak{t}_{\mathrm{ph}}(t,z)} \overline{A_{2\delta}(\mathfrak{t}_{\mathrm{gr}}(t,z))}\mathbf{R}(-\varphi_{\mathsf{F}}(t,z)) \cdot \mathbf{M}(t) \cdot \mathbf{R}(-\varphi_{\mathsf{F}}(t,z))\, dt.$$

  The integrand is constant: $\mathbf{I} = (\tau - 2\delta\tau)\mathbf{S}$ (no spatial dependence).

Distributed target: $\mathbf{S} = \mathbf{S}(z)$

- The received signal:

$$\mathbf{M}(t) = \int e^{-i\omega_0 \mathfrak{t}_{\mathrm{ph}}(t,z)} A_{2\delta}(\mathfrak{t}_{\mathrm{gr}}(t,z)) \mathbf{R}(\varphi_{\mathsf{F}}(t,z)) \cdot \mathbf{S}(z) \cdot \mathbf{R}(\varphi_{\mathsf{F}}(t,z))\, dz.$$

- The image is obtained by polarimetric matched filter (PMF):

$$\mathbf{I}(y) = \int \underbrace{e^{i\omega_0 \mathfrak{t}_{\mathrm{ph}}(t,y)} \overline{A_{2\delta}(\mathfrak{t}_{\mathrm{gr}}(t,y))}}_{\text{traditional scalar matched filter}} \mathbf{R}(-\varphi_{\mathsf{F}}(t,y)) \cdot \mathbf{M}(t) \cdot \mathbf{R}(-\varphi_{\mathsf{F}}(t,y))\, dt.$$

  The dependence of φ_{F} on t is assumed known (requires ω_{pe}, Ω_{e}).

- The imaging operator $\mathbf{S}(z) \mapsto \mathbf{I}(y)$:

$$\mathbf{I}(y) = \int dz\, e^{i\Phi} \int \overline{A_{2\delta}(\mathfrak{t}_{\mathrm{gr}}(t,y))} A_{2\delta}(\mathfrak{t}_{\mathrm{gr}}(t,z)) \mathbf{R}(\Delta\varphi_{\mathsf{F}}) \cdot \mathbf{S}(z) \cdot \mathbf{R}(\Delta\varphi_{\mathsf{F}})\, dt,$$

  where $\Phi = -2k_0(y-z)$, $k_0 = k(\omega_0)$, $\Delta\varphi_{\mathsf{F}} = \varphi_{\mathsf{F}}(t,z) - \varphi_{\mathsf{F}}(t,y)$.

The point spread function (PSF)

- The PSF is the kernel of the imaging operator:

$$W_{iklj}(y,z) = e^{i\Phi} \int \overline{A_{2\delta}(\mathfrak{t}_{\mathrm{gr}}(t,y))} A_{2\delta}(\mathfrak{t}_{\mathrm{gr}}(t,z)) R_{ik}(\Delta\varphi_{\mathsf{F}}) R_{lj}(\Delta\varphi_{\mathsf{F}}) dt,$$

so that $\quad I_{ij}(y) = \sum_{kl} \int W_{iklj}(y,z) S_{kl}(z)\, dz, \quad i,j,k,l \in \{\mathsf{H},\mathsf{V}\}.$

- In the case of single polarization, W is a scalar:
  - Ideally, one would want to have $W(y,z) \propto \delta(y-z)$;
  - In reality, it is not possible due to various constraints (bandwidth);
  - Practical systems are subject to limitations (resolution, sidelobes).
- In the quad-pol case, W is a rank 4 tensor:
  - The ideal form of its individual entries is still $W_{iklj} \propto \delta(y-z)$;
  - Polarimetric fidelity: are the different channels really separate?
  - The higher the fidelity, the closer the PSF to $W_{iklj} \propto \delta_{ik}\delta_{lj}$;
  - All other non-zero entries represent cross-channel contamination.
- In the presence of FR, there is always some contamination.

PMF vs. traditional polarimetry

- Traditional polarimetric reconstruction consists of two stages.
  1. Scalar matched filter is applied to individual channels:

$$Y_{pq}(y) = \int e^{i\omega_0 \mathrm{t}_{\mathrm{ph}}(t,y)} \overline{A_{2\delta}(\mathrm{t}_{\mathrm{gr}}(t,y))} M_{pq}(t)\, dt, \quad pq \in \{\mathrm{HH}, \mathrm{HV}, \mathrm{VH}, \mathrm{VV}\}.$$

  2. The rotation matrices are applied to intermediate images Y_{pq}:

$$\mathbf{I}_{\mathsf{trad}}(y) = \mathbf{R}(-\varphi_{\mathsf{F}}^*) \cdot \mathbf{Y}(y) \cdot \mathbf{R}(-\varphi_{\mathsf{F}}^*).$$

- The FR angle φ_{F}^* is constant as if the signal were monochromatic:

$$\varphi_{\mathsf{F}}^* = -\frac{\omega_{\mathrm{pe}}^2 \Omega_{\mathsf{e}}}{2c} \frac{R^*}{\omega_0^2}, \quad \text{where } R^* = z^* - x, \quad z^* \text{ is fixed.}$$

- The imaging operator is the same as before, but $\Delta\varphi_{\mathsf{F}}$ changes:

$$\Delta\varphi_{\mathsf{F}}^* = \varphi_{\mathsf{F}}(t,z) - \varphi_{\mathsf{F}}^*.$$

- Because of dFR, traditional PolSAR involves a filter mismatch:
  - It exists even for a known point scatterer: $\mathbf{S}(z) = \mathbf{S}_0 \delta(z - z_0)$;
  - Then, PMF is fully matched, but $\Delta\varphi_{\mathsf{F}}^* \neq 0$ for all t even if $z_0 = z^*$.
  - Then, $\mathbf{I}_{\mathsf{trad}}(z_0)$ may, e.g., have a non-zero entry where $\mathbf{S}_0$ has zero.

Equivalent 4×4 representation

- It is convenient to recast the imaging operator as follows:

$$\boldsymbol{I}(y) = \int \mathbf{W}(y,z) \cdot \boldsymbol{S}(z)\, dz,$$

where $\boldsymbol{I}(y) = (I_{\mathsf{HH}}, I_{\mathsf{HV}}, I_{\mathsf{VH}}, I_{\mathsf{VV}})^{\mathsf{T}}$, $\boldsymbol{S}(y) = (S_{\mathsf{HH}}, S_{\mathsf{HV}}, S_{\mathsf{VH}}, S_{\mathsf{VV}})^{\mathsf{T}}$, and

$$\mathbf{W}(y,z) = e^{i\Phi} \int \overline{A_{2\delta}(\mathfrak{t}_{\mathrm{gr}}(t,y))} A_{2\delta}(\mathfrak{t}_{\mathrm{gr}}(t,z)) \mathbf{V}(\Delta\varphi_{\mathsf{F}})\, dt,$$

$$\mathbf{V}(\phi) \overset{\mathsf{def}}{=} \begin{pmatrix} \cos^2\phi & -\cos\phi\sin\phi & \cos\phi\sin\phi & -\sin^2\phi \\ \cos\phi\sin\phi & \cos^2\phi & \sin^2\phi & \cos\phi\sin\phi \\ -\cos\phi\sin\phi & \sin^2\phi & \cos^2\phi & -\cos\phi\sin\phi \\ -\sin^2\phi & -\cos\phi\sin\phi & \cos\phi\sin\phi & \cos^2\phi \end{pmatrix}.$$

- The ideal form of the 4×4 matrices $\mathbf{V}(\Delta\varphi_{\mathsf{F}})$ and $\mathbf{W}(y,z)$ is diagonal, which is achieved if $\Delta\varphi_{\mathsf{F}} = 0$.
- In the presence of FR, this condition does not hold unless $y = z$.

Imaging kernel for the PMF

- The imaging kernel (recall, $\Delta\varphi_{\mathsf{F}} = \varphi_{\mathsf{F}}(t,z) - \varphi_{\mathsf{F}}(t,y)$):

$$\mathbf{W}(y,z) \approx \mathbf{V}\big(\Delta\varphi_{\mathsf{F}}(\omega_0)\big)e^{i\Phi} \underbrace{\int \overline{A_{2\delta}(\mathfrak{t}_{\rm gr}(t,y))}A_{2\delta}(\mathfrak{t}_{\rm gr}(t,z))\,dt}_{\text{encountered in the scalar case}}$$

$$\approx \mathbf{V}\big(\Delta\varphi_{\mathsf{F}}(\omega_0)\big)\underbrace{\tau e^{i\Phi}\chi_{B\tau}(\xi)\Big(1-\frac{2|\xi|}{B\tau}\Big)\operatorname{sinc}\Big[\xi\Big(1-\frac{2|\xi|}{B\tau}\Big)\Big]}_{W^{(B\tau)}(\xi) \text{ — PSF for single-channel imaging}},$$

  where $\xi = B(y-z)/v_{\rm gr}(\omega_0)$.
- The difference of rotation angles can be represented as

$$\Delta\varphi_{\mathsf{F}}(\omega_0) = \frac{2C_\tau}{B\tau}\eta\xi, \quad \text{where} \quad C_\tau = \mathcal{O}(1)$$

  and

$$\eta = \frac{|x|}{2c}\frac{\omega_{\rm pe}^2\Omega_{\mathsf{e}}}{\omega_0^2}\cdot\frac{2B}{\omega_0} \equiv -\varphi_{\mathsf{F}_0}\cdot\frac{2B}{\omega_0}$$

  is a typical scale of the total FR angle times relative bandwidth.

Imaging kernel for the PMF (cont'd)

- The 4×4 matrix $\mathbf{W}$ has only three different entries:

$$\mathbf{W} = \begin{pmatrix} W_0 & -W_1 & W_1 & -W_2 \\ W_1 & W_0 & W_2 & W_1 \\ -W_1 & W_2 & W_0 & -W_1 \\ -W_2 & -W_1 & W_1 & W_0 \end{pmatrix},$$

where

$$\begin{aligned} W_0(\xi,\eta) &= \cos^2\left(\frac{2C_\tau}{B\tau}\eta\xi\right) W^{(B\tau)}(\xi), \\ W_1(\xi,\eta) &= \cos\left(\frac{2C_\tau}{B\tau}\eta\xi\right)\sin\left(\frac{2C_\tau}{B\tau}\eta\xi\right) W^{(B\tau)}(\xi), \\ W_2(\xi,\eta) &= \sin^2\left(\frac{2C_\tau}{B\tau}\eta\xi\right) W^{(B\tau)}(\xi). \end{aligned}$$

- For high compression ratio: $B\tau \gg 1$, and $|\xi| \leqslant \pi$ (main lobe):

$$W_0 \approx \tau e^{i\Phi}\operatorname{sinc}\xi \quad \text{and} \quad |W_p| = \mathcal{O}\big(\tau \cdot (B\tau)^{-p}\big), \quad p = 0, 1, 2.$$

Performance of the PMF: scalar part

- Commonly used scalar metrics: resolution and ISLR.
- Resolution is semi-width of the main lobe; if $W \propto \operatorname{sinc}\xi$: $\Delta_{\mathrm{R}} = \dfrac{\pi c}{B}$.
- ISLR describes the spreading, i.e., geometric contamination:

$$\mathrm{ISLR}(W) = 10\log_{10}\left[\left(\int_{|\xi|>\pi} |W(\xi)|^2\, d\xi\right)\left(\int_{|\xi|\leqslant\pi} |W(\xi)|^2\, d\xi\right)^{-1}\right].$$

- For $W \propto \operatorname{sinc}\xi$, ISLR≈-9.68*dB* ⇒ 90% of energy in the main lobe.
- For the more general PSF $W^{(B\tau)}(\xi)$, we also have ISLR≈-9.7*dB*.
- For the matrix PSF $\mathbf{W}$, its diagonal entry $W_0 = \cos^2(\frac{2C_\tau}{B\tau}\eta\xi)W^{(B\tau)}(\xi)$.
- For the typical case of $|\eta| \lesssim 1$, ISLR(W_0) may differ by 0.1*dB*:
  - Hence, 90% of the total power of W_0 is in its main lobe as well.
- What about the vector metrics of performance?

Performance of the PMF: vector part

- Cross-channel contamination is due to off-diagonal entries of $\mathbf{W}$.
- Relative magnitude of the off-diagonal entries:

$$\|\mathbf{W}-\mathbf{D}\|\cdot\|\mathbf{D}\|^{-1}, \quad \text{where} \quad \mathbf{D} = \text{daig}\,\mathbf{W}.$$

- As $\mathbf{W} = \mathbf{W}(\xi,\eta)$, we integrate with respect to ξ:

$$\left(\int \|\mathbf{W}-\mathbf{D}\|^2 d\xi\right)\left(\int \|\mathbf{D}\|^2 d\xi\right)^{-1}$$
$$= \left(\int \left(2|W_1(\xi,\eta)|^2 + |W_2(\xi,\eta)|^2\right) d\xi\right)\left(\int |W_0(\xi,\eta)|^2 d\xi\right)^{-1},$$

and leave η as the parameter that characterizes the dFR effect:

  - Square of the Frobenius norm is used for convenience;
  - Superficially similar to what sits under the $\log$ in ISLR;
  - Integration limits will specify different metrics of contamination.

Point-based polarimetric contamination metric

- This metric, PPCM, is designed for point targets:
  - Quantifies the distortions in a given channel due to contributions from other channels at the same point (as opposed to sidelobes);
  - One should integrate over the main lobe of the diagonal entry:

$$\mathrm{PPCM}(\mathbf{W},\eta) = 10\log_{10}\left[\left(\int_{|\xi|\leqslant\pi} \left(2|W_1(\xi,\eta)|^2 + |W_2(\xi,\eta)|^2\right) d\xi\right) \cdot \left(\int_{|\xi|\leqslant\pi} |W_0(\xi,\eta)|^2 d\xi\right)^{-1}\right].$$

- For $|\eta| \lesssim 1$, the numerator is small, $\sim \pi\tau^2(B\tau)^{-2}$, because $B\tau \gg 1$.
- The denominator is $\sim 0.9\pi\tau^2$.
- For a sample P-band system, we take $B\tau = 2\pi \cdot 400$, which yields:

$$\mathrm{PPCM}(\mathbf{W},\eta) \approx -60dB.$$

- Negligible for all practical purposes.

Area-based polarimetric contamination metric

- This metric, APCM, is designed for distributed targets:
  - Intensity at a given point includes sidelobes of neighboring points;
  - To account for sidelobes, one should integrate over the entire real axis:
$$\text{APCM}(\mathbf{W},\eta) = 10\log_{10}\frac{2\|W_1\|_2^2(\eta)+\|W_2\|_2^2(\eta)}{\|W_0\|_2^2(\eta)}.$$
- The numerator is, again, small, but this time around, $\sim (B\tau)^{-1}$.
- Altogether,
$$\text{APCM}(\mathbf{W},\eta) \lesssim 10\log_{10}\left(\frac{1}{B\tau}\frac{4}{\pi}\left(2C_\tau^2\eta^2+\frac{1}{3}C_\tau^4\eta^4\right)\right).$$
- For the typical system parameters, this yields (even if $|\eta|\sim 1$):
$$\text{APCM}(\mathbf{W},\eta) \lesssim -30dB.$$
- For $|\eta| \ll 1$, the values of $\text{APCM}(\mathbf{W},\eta)$ are considerably smaller.
- Much larger than PPCM, yet still negligible for most practical purposes.

Performance of traditional polarimetry

- Uses a certain value of FR angle φ_{F}^{*} that is assumed constant.
- For arbitrary values of η:

$$\mathrm{APCM}(\mathbf{W},\eta) = 10\log_{10}\frac{5-\operatorname{sinc}2\eta-4\operatorname{sinc}\eta}{3+4\operatorname{sinc}\eta+\operatorname{sinc}2\eta}.$$

- For $|\eta| \ll 1$, this reduces to $\mathrm{APCM}(\mathbf{W},\eta) \approx 10\log_{10}\dfrac{\eta^2}{6}$.

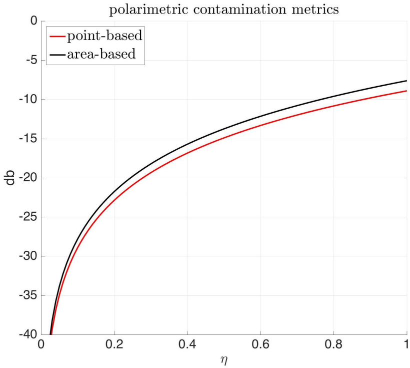

- PMF has a factor of $(B\tau)^{-1} \ll 1$.
- PPCM is obtained numerically.
- Polarimetric fidelity of the PMF is far superior to that of traditional polarimetry.
- Other metrics, beyond PPCM and APCM, may be useful.

Full-fledged PolSAR

- The space is 3D; the target is 2D.
- Aperture is synthesized by emitting identical pulses from equally spaced locations along the orbit, $\boldsymbol{x}^n = (x_1^n, -L, H)$, $|x_1^n| \le L_{\mathsf{SA}}/2$:

$$\begin{pmatrix} E_{\mathsf{H}}^{\mathsf{i}} \\ E_{\mathsf{V}}^{\mathsf{i}} \end{pmatrix}^n_{(\mathsf{H,V})} (t, \boldsymbol{x}^n) = \boldsymbol{E}_{(\mathsf{H,V})} A(t - t_n) e^{-i\omega_0 (t - t_n)}.$$

- The propagation direction is not necessarily parallel to the magnetic field $(\beta \neq 0) \Rightarrow$ there will be dFR in slow time t_n.
- Electron number density may vary with altitude, $N_{\mathsf{e}} = N_{\mathsf{e}}(h)$:

$$\varphi_{\mathsf{F}} = -\frac{\Omega_{\mathsf{e}} \cos\beta}{2c\omega^2 \cos\theta} \underbrace{\int_0^H \omega_{\text{pe}}^2(h)\, dh}_{\propto\ \mathsf{TEC}} = -\frac{R_z}{2c} \frac{\bar{\omega}_{\text{pe}}^2 \Omega_{\mathsf{e}} \cos\beta}{\omega^2}.$$

Full-fledged PolSAR (cont'd)

- Let $\boldsymbol{R}_z^n = \boldsymbol{z} - \boldsymbol{x}^n$, $R_z^n = |\boldsymbol{R}_z^n|$, and $\mathbf{e}_H = \boldsymbol{H}_0/|\boldsymbol{H}_0|$. Then,

$$\varphi_{\mathsf{F}}^n(t,\boldsymbol{z}) = -\frac{(\boldsymbol{R}_z^n, \mathbf{e}_H)}{2c} \frac{\bar{\omega}_{\text{pe}}^2 \Omega_{\mathsf{e}}}{\omega^2(t - 2R_z^n/\bar{v}_{\text{gr}}(\omega_0))}.$$

- The received signal for monostatic imaging:

$$\mathbf{M}(t,\boldsymbol{x}^n) = \chi_{L_{\mathsf{SA}}}(x_1^n - z_1) \int e^{-i\omega_0 \mathfrak{t}_{\text{ph}}^n(t,\boldsymbol{z})} A(\mathfrak{t}_{\text{gr}}^n(t,\boldsymbol{z})) \\ \mathbf{R}(\varphi_{\mathsf{F}}^n(t,\boldsymbol{z})) \cdot \mathbf{S}(\boldsymbol{z}) \cdot \mathbf{R}(\varphi_{\mathsf{F}}^n(t,\boldsymbol{z}))\, d\boldsymbol{z}.$$

- The image is obtained by means of a filter that matches the phase and rotation angle of the received signal in fast and slow time:

$$\mathbf{I}(\boldsymbol{y}) = \sum_n \chi_{L_{\mathsf{SA}}}(x_1^n - y_1) \int e^{i\omega_0 \mathfrak{t}_{\text{ph}}^n(t,\boldsymbol{y})} \overline{A(\mathfrak{t}_{\text{gr}}^n(t,\boldsymbol{y}))} \\ \mathbf{R}(-\varphi_{\mathsf{F}}^n(t,\boldsymbol{y})) \cdot \mathbf{M}(t,\boldsymbol{x}^n) \cdot \mathbf{R}(-\varphi_{\mathsf{F}}^n(t,\boldsymbol{y}))\, dt.$$

Full-fledged PolSAR (cont'd)

- The imaging operator:

$$\boldsymbol{I}(\boldsymbol{y}) = \int \mathbf{W}(\boldsymbol{y},\boldsymbol{z}) \cdot \boldsymbol{S}(\boldsymbol{z})\, d\boldsymbol{z}.$$

- The kernel is factorized:

$$\mathbf{W}(\boldsymbol{y},\boldsymbol{z}) = \mathbf{V}(\Delta\varphi_{\mathsf{F}}) e^{i\Phi_0} W_{\mathsf{A}}(\xi_{\mathsf{A}}) W_{\mathsf{R}}(\xi_{\mathsf{R}}),$$

where

$$\begin{aligned} W_{\mathsf{A}}(\xi_{\mathsf{A}}) &= \chi_{4\pi\mathfrak{F}}(\xi_{\mathsf{A}}) N\left(1 - \frac{|\xi_{\mathsf{A}}|}{2\pi\mathfrak{F}}\right) \operatorname{sinc}\left[\xi_{\mathsf{A}}\left(1 - \frac{|\xi_{\mathsf{A}}|}{2\pi\mathfrak{F}}\right)\right], \\ W_{\mathsf{R}}(\xi_{\mathsf{R}}) &= \chi_{B\tau}(\xi_{\mathsf{R}}) \tau\left(1 - \frac{2|\xi_{\mathsf{R}}|}{B\tau}\right) \operatorname{sinc}\left[\xi_{\mathsf{R}}\left(1 - \frac{2|\xi_{\mathsf{R}}|}{B\tau}\right)\right], \end{aligned}$$

$\Phi_0 = -2k_0(y_2 - z_2)\sin\theta$, $\xi_{\mathsf{A}} = \frac{k_0(y_1 - z_1)L_{\mathsf{SA}}}{R}$, $\xi_{\mathsf{R}} = \frac{B(y_2 - z_2)\sin\theta}{\bar{v}_{\text{gr}}(\omega_0)}$, and $\mathfrak{F} = L_{\mathsf{SA}}^2/(R\lambda_0)$ is the Fresnel number for the aperture of size L_{SA}.

- $\Delta\varphi_{\mathsf{F}} \approx \frac{1}{2\pi\mathfrak{F}}\eta_{\mathsf{A}}\xi_{\mathsf{A}} + \frac{2C_{\mathsf{R}}}{B\tau}\eta\xi_{\mathsf{R}}$, where $\eta_{\mathsf{A}} = -\varphi_{\mathsf{F}_0}(\mathbf{e}_{\boldsymbol{H}}, \mathbf{e}_1)\frac{L_{\mathsf{SA}}}{R}$, $C_{\mathsf{R}} \approx 1$.

Performance estimates

- ACPM for the PMF in the case of a full-fledged PolSAR:

$$\mathsf{APCM}(\mathbf{W}, \eta_\mathsf{A}, \eta) \sim 10\log_{10}\left[\max\left(\frac{\eta_\mathsf{A}^2}{\mathfrak{F}}, \frac{C_\mathsf{R}^2\eta^2}{B\tau}, \frac{\eta_\mathsf{A}^4}{\mathfrak{F}}, \frac{C_\mathsf{R}^4\eta^4}{B\tau}\right)\right].$$

  Represents the "worst case scenario" as PPCM is (much) smaller.
- For $|\eta_\mathsf{A}| \sim |\eta| \lesssim 1$ and $\mathfrak{F} \sim B\tau \gg 1$, the resulting estimate is roughly the same as that for the single-pulse imaging.

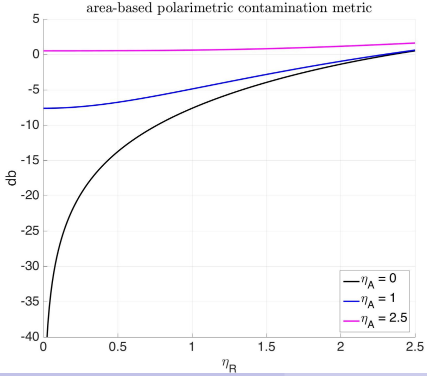

- The key conclusion stays: PMF yields low level of distortions.
- For traditional PolSAR, the error (APCM) is significant if at least one of the dFR parameters, $|\eta_\mathsf{A}|$ or $|\eta_\mathsf{R}|$, is not small.
- Again, polarimetric fidelity of the PMF is far superior to that of traditional PolSAR.

Discussion: what do those decibels mean?

- As a minimum, the reflectivity in a given channel should contribute mostly to the received signal in the same channel:

$$\|W_1\|_2^2 \ll \|W_0\|_2^2, \quad \|W_2\|_2^2 \ll \|W_0\|_2^2.$$

  Hence, APCM should be a sufficiently large negative number.
- Polarimetric applications. The reflectivity in different channels may differ by up to 10*dB*. To prevent contamination by a stronger channel, the threshold should be reduced further:

$$\text{APCM}(\mathbf{W}) \ll -10dB.$$

- Applications of PolSAR interferometry. The bare soil reflectivity in one channel may be 20 to 30*dB* smaller than that from vegetation in a different channel. This lowers the threshold even further:

$$\text{APCM}(\mathbf{W}) \ll -20dB.$$

Discussion (cont'd)

- For a P-band system, $\omega_0/2\pi = 300MHz$, $B/2\pi = 8MHz$, $\tau = 5 \cdot 10^{-5}s$, $\theta = 60^\circ$, and relatively high TEC of $5 \cdot 10^{13} cm^{-2}$, the error of the traditional PolSAR reconstruction is (for a specific direction of $\boldsymbol{H}_0$):

$$\text{APCM}(\mathbf{W}) \approx -11dB.$$

- PMF will reduce APCM by $\sim 10 \log_{10} B\tau$, i.e., by more than 30*dB*.
- The contemplated BIOMASS mission:

$$\omega_0/2\pi = 435MHz, \quad B/2\pi = 6MHz, \quad H = 670km, \quad \theta = 30^\circ.$$

- For traditional PolSAR we obtain a borderline value of

$$\text{APCM}(\mathbf{W}) \approx -25dB.$$

- Yet the PMF will put APCM safely below all thresholds.
- More subtle criteria may be needed, to handle the odd/even nature of the various entries of $\mathbf{W}$ — double intensity peaks.